

Thermal diffusivity of fluid oxygen to 12 GPa and 300°C

E. H. Abramson, L. J. Slutsky, and J. M. Brown

Citation: *The Journal of Chemical Physics* **111**, 9357 (1999); doi: 10.1063/1.479849

View online: <http://dx.doi.org/10.1063/1.479849>

View Table of Contents: <http://scitation.aip.org/content/aip/journal/jcp/111/20?ver=pdfcov>

Published by the [AIP Publishing](#)

Articles you may be interested in

[Equation of State for Solid Phase I of Carbon Dioxide Valid for Temperatures up to 800 K and Pressures up to 12 GPa](#)

J. Phys. Chem. Ref. Data **40**, 043105 (2011); 10.1063/1.3664915

[Equation of state and anharmonicity of carbon dioxide phase I up to 12 GPa and 800 K](#)

J. Chem. Phys. **133**, 144501 (2010); 10.1063/1.3495951

[Experimental and theoretical studies on the elasticity of molybdenum to 12 GPa](#)

J. Appl. Phys. **106**, 043506 (2009); 10.1063/1.3197135

[Perturbation Method for Study of Shear Strength of Materials at Pressures up to 300 GPa](#)

AIP Conf. Proc. **845**, 745 (2006); 10.1063/1.2263430

[Quasisentropic Compressibility of Gaseous Deuterium in Pressure Range up to 300 GPa](#)

AIP Conf. Proc. **706**, 73 (2004); 10.1063/1.1780187



Thermal diffusivity of fluid oxygen to 12 GPa and 300 °C

E. H. Abramson^{a)} and L. J. Slutsky

Department of Chemistry, University of Washington, Seattle, Washington 98195

J. M. Brown

Geophysics Program, University of Washington, Seattle, Washington 98195

(Received 22 July 1999; accepted 31 August 1999)

The thermal diffusivity of fluid oxygen in the diamond-anvil cell has been measured from 1 to 12.6 GPa and 25 to 300 °C. These constitute the first experimental measurements of thermal transport properties of simple fluids above 1 GPa. Diffusivities are found to rise sharply from a minimum at intermediate pressures and then to level off at ~6 GPa. Thermal conductivities derived from these measurements do not vary as \sqrt{T} , rather the excess conductivities are approximately independent of temperature. The diffusivities of nitrogen, previously measured to 1 GPa, closely match those of oxygen when scaled as suggested by a simple, corresponding states theory. © 1999 American Institute of Physics. [S0021-9606(99)51344-5]

INTRODUCTION

Measurements of the thermal transport coefficients of simple fluids have been reported only up to pressures of 1 GPa,^{1,2} corresponding to densities of ~0.7 of the close-packed value based on a Lennard-Jones σ . Transport properties at considerably higher density play a central role in the construction of planetary models³ and in the modeling of detonations. Moreover, analysis of the temperature dependence of diffusion coefficients, viscosity, and thermal conductivity has traditionally been an important experimental constraint on intermolecular potential functions. We report here measurements of the thermal diffusivity of fluid oxygen in the strongly repulsive region. Pressures extend to 12.6 GPa, temperatures from 25 °C to 300 °C. Densities significantly higher than the nominal Lennard-Jones close-packed value are achieved. The temperature dependence of the thermal conductivity derived from hard-sphere models and observed at lower density does not describe these high-pressure results.

EXPERIMENT

Liquid oxygen (>99.99%) is loaded into a Merrill-Basset diamond-anvil cell with a hardened, Inconel 718 gasket and enclosed in a temperature-controlled, vacuum furnace. The pressure is determined by comparison of the wavelength of the maximum in the R1 fluorescence of a ruby chip⁴ within the cell with that of another ruby at the same temperature; it is assumed that the pressure variation of the fluorescence wavelength is independent of temperature.²⁰

Two 1064 nm pulses, of ~80 ps duration and ~10 μ J, selected from the output train of a Q-switched, mode-locked, Nd-YAG laser, are recombined at angle 2θ in the fluid. Interference produces a spatially periodic distribution of intensity in the sample. Absorption of the light results in a periodic distribution of electronic and vibrational excitation, and

a spatially periodic distribution of temperature and hence of index of refraction ensues. The period, d , of the resultant grating in terms of the laser wavelength, λ_{IR} , is

$$d = \frac{\lambda_{\text{IR}}}{2 \sin \theta}. \quad (1)$$

The intensity of the Bragg-scattering of a five milliwatt argon-ion laser probe, detected by a photomultiplier and averaged by a Tektronix 2430 oscilloscope serves to monitor the evolution of the grating created by the crossed excitation pulses. In the case of one-dimensional thermal conduction in an optically thin, thermally thick sample, the rate constant, R , and relaxation time, τ , for the exponential decay of the periodic distribution of temperature are given by

$$R = \frac{1}{\tau} = \frac{4\pi^2 D}{d^2}, \quad (2)$$

where D is the thermal diffusivity (that is, the thermal conductivity divided by the isobaric heat capacity per unit volume); the decay rate of the signal is $2R$. The variation of R with the angle of intersection, specified by Eqs. (1) and (2), distinguishes one-dimensional thermal diffusion from other relaxation processes. The value of d was varied between 2.5 and 7 μ m; the sample thickness was at least a factor of ten greater than d for all measurements, with the exception of those points at the two highest pressures for which the ratio of distances was larger than eight. The maximum temperature rise of the fluid due to the laser pulses is estimated to be less than 1 °C and is negligible.

The thermal diffusivity determined in this way has, above 2 GPa, a usual scatter of $\pm 1\%$. At ambient pressure and room temperature, results for water^{5,6} and methanol⁶ agree with other methods within 1.5%. For oxygen in the diamond-anvil cell below 2 GPa the Bragg-diffracted signal is weak and, unlike the situation at higher pressures, the decay of electronic and vibrational excitation is not extremely rapid compared with the relaxation time of the thermal grating; our point of lowest density at 1.2 GPa and 300 °C, has

^{a)}Electronic mail: evan@geophys.washington.edu

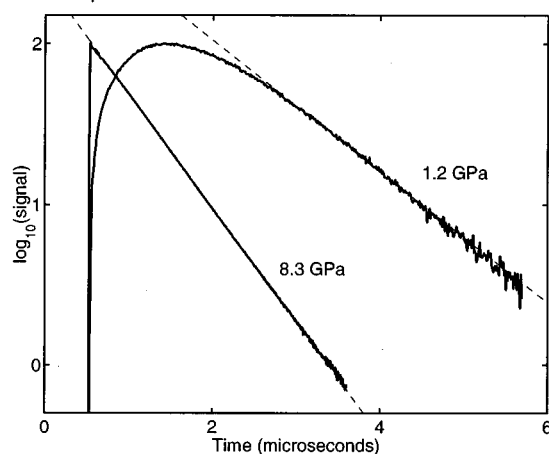


FIG. 1. Semilog plots of the signal intensity as a function of time for two traces at 300 °C and pressures of 8.3 and 1.2 GPa. The low-pressure data show an ingrowth of the signal due to a slow relaxation of the initial excitation; this trace represents our least favorable experimental situation. Straight, dashed lines are fits through the data.

an estimated uncertainty of $\pm 5\%$. Semilog plots of a typical signal at 8.3 GPa and also the signal at lowest density, referred to above, are shown in Fig. 1.

RESULTS

The thermal diffusivity of fluid oxygen at 298, 473, and 573 K is plotted as a function of pressure in Fig. 2; at these temperatures the freezing points are, respectively, 5.8, 10.5, and 13.2 GPa. The pressure derivatives of the diffusivities decrease sharply with pressure and, for the data at 473 and 573 K the diffusivities level off to an approximately constant value.

In Fig. 3 the same data are plotted as functions of density. For this purpose the densities are taken from Ref. 7 (based on the speed of sound at 303 and 473 K) and extrapolated as necessary. The thermal diffusivities at 298 K of crystalline β -oxygen¹⁰ parallel and perpendicular to the c axis of the hexagonal unit cell are also shown; they are considerably larger than those of the fluid at comparable density. Lower

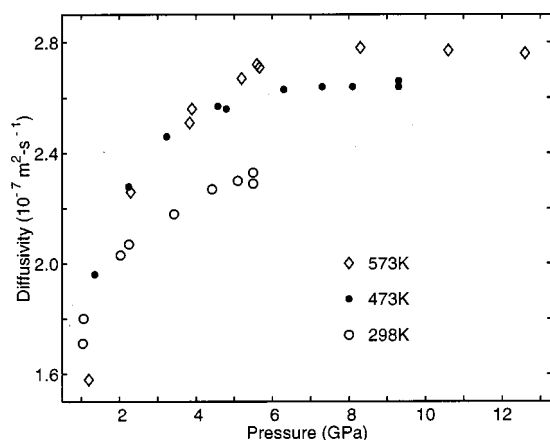


FIG. 2. The thermal diffusivity of fluid oxygen at 298, 473, and 573 K as a function of pressure.

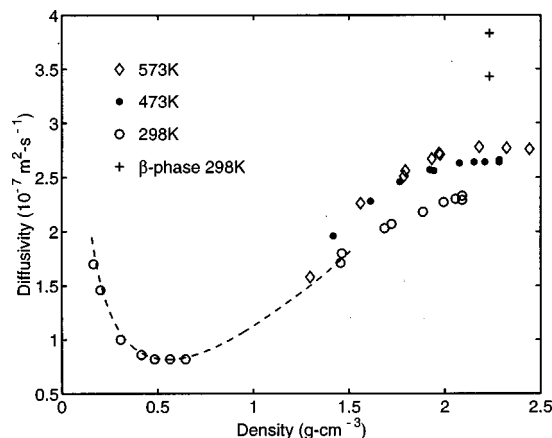


FIG. 3. The thermal diffusivity of fluid oxygen at 298, 473, and 573 K as a function of density. The points at low density are reported by H. Roder (Ref. 11). The thermal diffusivity of solid, β -oxygen at 298 K, along and perpendicular to the c axis, is also shown. The dashed curve represents results for nitrogen at 298 K, scaled as indicated in Eq. (4).

pressure data, from a study of the fluid¹¹ up to 70 MPa and 310 K, are plotted in the same figure along a 298 K isotherm.

The calculation of thermal conductivity (λ) from the directly measured diffusivity rests on the equation of state derived from acoustic data.⁷ In particular the heat capacity at high pressure is calculated starting from values at moderate pressure^{8,9} by integration of

$$\left(\frac{\partial C_p}{\partial P} \right)_T = -T \left(\frac{\partial^2 V}{\partial T^2} \right)_P, \quad (3)$$

where C_p is the specific heat and V the specific volume. This procedure requires knowledge of a second derivative with respect to T at pressures where the temperature dependence of both the velocity of sound and the volume is small. The possible error in λ is principally from this source and, while difficult to estimate, is judged by the consequence of adopting alternate procedures for fitting the acoustic data to be about 10%.

DISCUSSION

In both planetary science and in the modeling of detonation processes, estimates of viscosity and density as well as the thermal conductivity are important. To the extent that the internuclear potential is known, simulation and the Green-Kubo formulation or, alternately, nonequilibrium molecular dynamics provide computational routes to these properties at genuinely extreme conditions where experimentation is not at present practical. Data presented in this paper and the attendant measurements of the velocity of sound⁷ offer an opportunity to confront model potentials with experiment in the high-density regime.

Alternately, computationally undemanding schemes, based on corresponding states and on scaling methods suggested by hard-sphere models, have been successful to $\rho/\rho_0 \approx 0.7$, where ρ_0 is the close-packed density. For oxygen, an appropriate hard-sphere diameter (often approximated by the Lennard-Jones σ) is $\sigma \approx 3.41 \text{ \AA}$ and the nominal close-packed density, $\rho_0 = \sqrt{2}/\sigma^3$, is equivalent to 1.89 g cm^{-3} . The

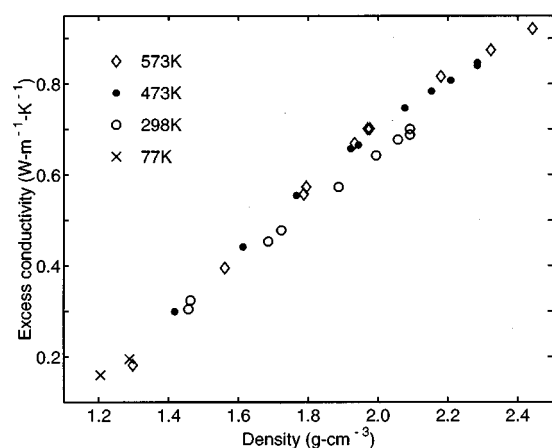


FIG. 4. The excess thermal conductivity of fluid oxygen at 77 K (from Ref. 11), 298, 473, and 573 K as a function of density.

measurements reported here then probe reduced densities ρ/ρ_0 of between 0.7 and 1.3. The present data serve to delineate the range of utility of these simpler approaches to the estimation of transport properties at high densities.

At intermediate densities the modified Enskog theory¹² (in conjunction with dynamical simulations^{13–15} of Lennard-Jones or hard-sphere systems) has served to rationalize and correlate the temperature and density dependence of the transport coefficients of simple molecules. Within the context of this theory, at fixed temperature, $\lambda\sigma^2\sqrt{m}$ is a universal function of ρ/σ^3 , where ρ , λ , and m are, respectively, the molar density, the conductivity and the molar mass. In terms of corresponding states, results for oxygen at density ρ are properly compared to those for nitrogen at $\rho[\rho^{\text{crit}}(\text{N}_2)/\rho^{\text{crit}}(\text{O}_2)]$, an appropriate scaling being

$$\lambda(\text{O}_2) = \lambda(\text{N}_2) \sqrt{\frac{28}{32}} \left(\frac{\rho^{\text{crit}}(\text{O}_2)}{\rho^{\text{crit}}(\text{N}_2)} \right)^{2/3}, \quad (4)$$

where ρ^{crit} represents the critical density. The dotted line in Fig. 3 represents the result of scaling the thermal conductivity of nitrogen,¹⁶ measured to 1 GPa at 298 K by Tufeu and Le Neindre¹⁷ as indicated by Eq. (4), the values of C_p and ρ required for the calculation of diffusivities being taken from Refs. 18 and 19. The range of overlap with the present high-pressure data is not large, but the concept of corresponding states would appear in this case to be quite successful.

Enskog theory also implies that, at constant density, the thermal conductivity and viscosity are proportional to \sqrt{T} as they are for the tenuous gas. It has, however, been observed that at intermediate pressures the excess thermal conductivity, $\lambda - \lambda^\circ$ (with λ° the limiting value as the pressure is reduced), is approximately independent of the temperature.¹² The extension of such scaling relations or empirical relations to higher densities would, if valid, be quite useful.

The excess thermal conductivity at 77, 298, 473, and 573 K is plotted versus density in Fig. 4, with λ° taken as the value at 1 bar. For our high-pressure data λ° at the lowest densities displayed is $\sim 25\%$ of the experimental value of λ , at the highest densities 5%. Both the configurational heat capacity and density decrease with increasing temperature so

the temperature dependence of λ seen in Fig. 4 is somewhat less than that exhibited by D . It is clear that to assume that λ is proportional to \sqrt{T} would considerably overestimate the modest temperature dependence of the thermal conductivity at constant high density.

SUMMARY

These measurements extend, for one simple fluid, studies of thermal transport to a higher range of pressures and densities than has, in the past, been readily subject to investigation. At the highest pressures mean intermolecular separations are in the strongly repulsive regime. Comparison of thermal conductivities of oxygen derived from the present data with results for nitrogen at somewhat lower pressure and density suggest that, at least for the symmetrical diatomics, scaling based on corresponding states is a reasonably successful procedure. Below 6 GPa, the thermal diffusivity increases with increasing pressure; between 6 and 12.6 GPa the diffusivity is independent of pressure to within an experimental error of 2%. The temperature dependence of the excess thermal conductivity is small throughout the range of densities spanned by these data. The thermal diffusivity of the fluid at 25 °C is about 60% of that of crystalline oxygen at the same temperature and density.

ACKNOWLEDGMENTS

This work was supported by Grant Nos. EAR 96-14313 and EAR 98-14599 from the National Science Foundation and by research subcontract B5030002 from Lawrence Livermore National Laboratory.

- ¹A. Michels, J. V. Sengers, and L. J. M. van der Kleindert, *Physica (Amsterdam)* **29**, 149 (1963).
- ²B. Le Neindre, Y. Garrabos, and R. Tufeu, *Physica A* **156**, 512 (1989).
- ³D. J. Stevenson and E. E. Salpeter, *Astrophys. J., Suppl.* **35**, 221 (1977).
- ⁴H. K. Mao, P. M. Bell, J. W. Shaner, and D. J. Steinberg, *J. Appl. Phys.* **49**, 3276 (1978).
- ⁵M. L. V. Ramires, C. A. Nieto de Castro, Y. Nagasaka, A. Nagashim, M. J. Assael, and W. A. Wakeham, *J. Phys. Chem. Ref. Data* **24**, 1377 (1995).
- ⁶M. J. Assael, E. Charitidou, G. P. Georgiadis, and W. A. Wakeham, *Ber. Bunsenges. Phys. Chem.* **92**, 627 (1998).
- ⁷E. H. Abramson, L. J. Slutsky, M. D. Harrell, and J. M. Brown, *J. Chem. Phys.* **110**, 10493 (1999).
- ⁸W. Wagner, K. M. de Reuck, and S. Angus, *Oxygen: International Thermodynamic Tables of the Fluid State 9* (Blackwell Scientific, Oxford, 1987).
- ⁹L. A. Weber, NASA reference publication Report No. 1011 NBSIR 77-865 (1977).
- ¹⁰E. H. Abramson, L. J. Slutsky, and J. M. Brown, *J. Chem. Phys.* **104**, 5424 (1996).
- ¹¹H. M. Roder, *J. Res. Natl. Bur. Stand.* **87**, 279 (1982).
- ¹²W. A. Wakeham, in *Transport Properties of Fluids*, edited by J. Millat, J. H. Dymond, and C. A. Nieto de Castro (Cambridge University Press, Cambridge, 1996), pp. 83–88.
- ¹³C. Hoheisel, Computer Calculations, in *Transport Properties of Fluids*, edited by J. Millat, J. H. Dymond, and C. A. Nieto de Castro (Cambridge University Press, Cambridge, 1996), pp. 189–209.
- ¹⁴B. J. Alder, D. M. Gass, and T. E. Wainwright, *J. Chem. Phys.* **53**, 3813 (1970).
- ¹⁵R. Vogelsang and C. Hoheisel, *Phys. Chem. Liq.* **16**, 189 (1987).

- ¹⁶K. Stephan, R. Krause, and A. Laesecha, J. Phys. Chem. Ref. Data **16**, 993 (1989).
- ¹⁷R. Tufeu and B. Le Neindre, Int. J. Thermophys. **1**, 375 (1980).
- ¹⁸S. Angus, K. M. de Reuck, and B. Armstrong, *International Thermodynamic Tables of the Fluid State-6: Nitrogen* (Pergamon, Oxford, 1979).
- ¹⁹R. L. Mills, D. H. Liebenberg, and J. C. Bronson, J. Chem. Phys. **63**, 1198 (1975).
- ²⁰S. Wiryana, L. J. Slutsky, and J. M. Brown, Earth Planet. Sci. Lett. **163**, 123 (1998).